Y. Diboune, R. Hachelaf, D. Kouchih

Effect of short-circuit in stator windings on the operation of doubly-fed induction generators operating in a wind power system

Introduction. Wind energy has been a clean and renewable source of electricity in recent decades, making a significant addition to overall generation, and wind power is one of the most popular sources of renewable energy. Problem. Accurate modeling of wind turbine generators is critical to improve the efficiency of power systems. Doubly-fed induction generator (DFIG) stands out for its economic advantages associated with the use of frequency converters and induction machines. Increasing operating and maintenance costs of wind turbines highlight the need for early fault identification to optimize costs and ensure reliable operation. The goal of this work is to develop a simplified yet effective model for analyzing stator winding short-circuits in DFIGs operating in wind turbines. The model uses line-to-line voltages as inputs and explicitly considers the neutral-point voltage variation under fault conditions. Methodology. The problem was solved using spectral analysis, the model was implemented for 4 kW DFIG wind turbine in MATLAB to validate its effectiveness. Results. The simulation results confirm the effectiveness of the proposed approach for timely fault detection and analysis. It demonstrates computational simplicity by accurately capturing the main fault characteristics, which is preferable to traditional methods such as symmetrical components and FEM. The scientific novelty of the work lies in a methodology for modeling DFIG during stator short-circuits, integrating the effect of elevated neutral voltage during faults using line-to-line voltages in the base model. It also takes into account phenomena such as magnetic saturation, gap effects, and skin effects. The simplicity of the model makes it suitable for condition monitoring and validation of fault-tolerant control algorithms, which distinguishes it from more complex methods such as symmetrical components or the FEM. Practical value. The proposed model offers a pragmatic and reliable approach for monitoring and analyzing defects in DFIG wind turbines. Its versatility and efficiency improve the optimization of maintenance costs and reliability of renewable energy systems. References 27, tables 2, figures 8.

Key words: doubly-fed induction generator, short-circuit fault, wind turbine.

Вступ. Вітроенергетика є екологічно чистим та відновлюваним джерелом електроенергії в останні десятиліття, роблячи значний внесок у загальну генерацію енергії, і є одним із найпопулярніших джерел відновлюваної енергії. Проблема. Точне моделювання вітрогенераторів ϵ критично важливим для підвищення ефективності енергосистем. Асинхронний генератор з подвійним живленням (DFIG) відрізняється економічними перевагами, пов'язаними з використанням перетворювачів частоти та асинхронних машин. Зростання витрат на експлуатацію та технічне обслуговування вітрогенераторів призводить до необхідності раннього виявлення несправностей для оптимізації витрат та забезпечення надійної роботи. Метою даної роботи є розробка спрощеної, але ефективної моделі для розрахунку короткого замикання обмотки статора DFIG, що працює у вітрогенераторі. Модель використовує значення лінійної напруги та враховує підвищення напруги в нейтральній точці у разі несправностей. Методика. Завдання вирішено за допомогою спектрального аналізу. Модель реалізована у MATLAB для вітрогенератора DFIG потужністю 4 кВт для підтвердження її ефективності. **Результати** моделювання підтверджують ефективність запропонованого підходу до своєчасного виявлення та аналізу несправностей. Модель демонструє обчислювальну простоту, точно фіксуючи основні характеристики несправностей, що краще традиційних методів, таких як симетричні компоненти та метод скінченних елементів (МСЕ). Наукова новизна роботи полягає в методології моделювання DFIG при коротких замиканнях статора, що враховує вплив підвищеної напруги нейтралі при коротких замиканнях з використанням лінійних напруг базової моделі. Модель також враховує такі явища, як магнітне насичення, вплив зазору та скін-ефект. Простота моделі робить її придатною для моніторингу стану та валідації алгоритмів стійкості до відмови, що відрізняє її від складніших методів, таких як симетричні компоненти або МСЕ. Практична значимість. Розроблена модель пропонує практичний та надійний підхід до моніторингу та аналізу дефектів у вітрових турбінах з DFIG. Її універсальність та ефективність сприяють оптимізації витрат на технічне обслуговування та підвищенню надійності систем відновлюваної енергетики. Бібл. 27, табл. 2, рис. 8.

Ключові слова: асинхронний генератор з подвійним живленням, коротке замикання, вітрова турбіна.

Introduction. Wind energy is recognized as one of the most efficient and resilient renewable energy sources. In modern power systems, the configuration of variable-speed wind turbines is widely adopted to maximize energy capture and operational flexibility. Among the components of wind energy conversion systems, doubly-fed induction generators (DFIGs) are preferred due to their capability for variable-speed constant-frequency operation and high system efficiency [1].

The stator windings of DFIGs are subjected to thermal, electrical, and mechanical stresses, which can affect the performance and reliability of the generator and associated components [2, 3]. Inter-turn short circuit faults in the stator windings are particularly critical because they disturb voltage and current symmetry, potentially destabilizing the entire system [4]. Compared to other generator types used in wind energy, squirrel-cage induction generators operate only at fixed speed and lack controllability [5], while permanent magnet synchronous generators offer high efficiency but

require full-scale converters and are more expensive [6]. DFIGs remain a practical compromise for medium and high power applications due to their partial converter rating and grid compatibility.

Several techniques have been developed for detecting inter-turn short-circuit faults in the stator windings of DFIG-based wind energy systems. Signal-based methods remain prevalent, where fault diagnosis is performed by monitoring deviations in physical quantities such as external leakage flux [7], wideband frequency response [8], flux density distribution [9], and vibration analysis [10]. However, selecting an appropriate monitoring signal remains a key challenge, especially in distinguishing stator asymmetries. Observer-based approaches have also been applied [11], yet they may suffer from parameter sensitivity and false positives. Recently, artificial intelligence methods including neural networks [12], deep learning [13] and decision trees [14] have shown potential for fault

© Y. Diboune, R. Hachelaf, D. Kouchih

classification, although they are often complex and require extensive training data. For modeling stator winding short-circuit faults, classical techniques such as the symmetrical components method [15] and finite element method (FEM) [16–18] are commonly used. However, both approaches tend to overlook the neutral-point voltage rise during fault conditions and require considerable simulation time.

This study focuses on small-scale wind energy systems using DFIGs rated at 4 kW [19], primarily designed for stand-alone applications or isolated consumers.

The **goal** of this work is to develop a simplified yet effective model for analyzing stator winding short-circuits in DFIGs operating in wind turbines. The model uses line-to-line voltages as inputs and explicitly considers the neutral-point voltage variation under fault conditions.

This formulation enables efficient fault detection and analysis, supporting the development of condition monitoring strategies and fault-tolerant control schemes. Spectrum analysis is used to extract key harmonic indicators related to stator faults and validate the model through simulation on a 4 kW system.

Turbine modeling. The blades of a wind turbine capture the kinetic energy of the wind and transmit it to the rotor of a DFIG via a gearbox [20]. The wind turbine's power is calculated as:

$$P_{v} = \frac{1}{2} \cdot \rho \cdot S \cdot v^{2} \,, \tag{1}$$

where P_{ν} is the wind turbine's power; S is the surface swept by the blades of the turbine; ρ is the air density; ν is the wind speed.

The wind turbine's mechanical power is expressed as [21, 22]:

$$P_t = \frac{1}{2} \cdot \rho \cdot S \cdot C_p(\lambda, \beta) \cdot v^3, \qquad (2)$$

where P_t is the mechanical power; $C_p(\lambda, \beta)$ is referred to as the power coefficient, indicating the turbine aerodynamic efficiency. It depends on the tip speed ratio λ , defined as the quotient of the blade tip speed to the wind speed, and the blade pitch angle β .

The ratio λ can be articulated as [23, 24]:

$$\lambda = R \cdot \Omega_t / v \,, \tag{3}$$

where Ω_t is the rotational speed of the turbine; R is the blade radius.

The function of the power coefficient is (4):

$$C_p(\lambda, \beta) = 0.35 - 0.0167(\beta - 2)\sin\left(\frac{\pi \cdot (\lambda + 0.1)}{14.34 - 0.3(\beta - 2)}\right).$$
 (4)

Aerodynamic torque T_t is produced when aerodynamic power is transformed into mechanical power [25]:

$$T_t = \frac{P_t}{\Omega_t} = \frac{1}{2 \cdot \Omega_t} \cdot \rho \cdot S \cdot C_p(\lambda, \beta) \cdot v^3.$$
 (5)

The gearbox is a speed adapter from that of the turbine to that of the generator [26]:

$$G = T_t / T_m = \Omega_m / \Omega_t , \qquad (6)$$

where Ω_m is the mechanical speed; T_m is the mechanical torque.

Finally applying the fundamental relation of the dynamic, the model is completed as:

$$J\frac{\mathrm{d}\Omega_m}{\mathrm{d}t} = T_m - T_{em} - f_v \cdot \Omega_m, \tag{7}$$

where J is the total inertia; T_{em} is the electromagnetic torque; f_v is the viscous friction.

DFIG modeling. Under asymmetrical conditions, the stator voltages are unknown and deviate from the network phase voltages due to fluctuations in the neutral point voltage. This effect entails utilizing line-to-line voltages as inputs in the state model of the DFIG [19]. Thus, the stator voltage is indicated as:

$$\frac{\mathrm{d}[\boldsymbol{\Phi}_{sc}]}{\mathrm{d}t} = [\boldsymbol{U}_{sc}] + [\boldsymbol{R}_{sc}] \cdot [\boldsymbol{i}_{sc}], \tag{8}$$

where $[\boldsymbol{\Phi}_{sc}]$ is the stator fluxes vector; $[\boldsymbol{U}_{sc}] = [U_{ab}, U_{bc}, U_{ca}, 0]^T$ is the line voltages vector; $[\boldsymbol{i}_{sc}] = [i_{as}, i_{bs}, i_{cs}, i_{d}]^T$ is the line currents vector; $[\boldsymbol{R}_{sc}]$ is the stator windings resistances matrix:

$$\begin{bmatrix} R_{sc} \end{bmatrix} = \begin{bmatrix} r_{as} & -r_{bs} & 0 & 0 \\ 0 & r_{bs} & -r_{cs} & 0 \\ -r_{as} & 0 & r_{cs} & 0 \\ 0 & 0 & 0 & r_{d} \end{bmatrix}.$$
(9)

A short-circuit between 2 distinct places in the stator windings creates an alternative short-circuited phase, designated as «d» [27]. The novel phase is represented as:

$$r_d \cdot i_d + \frac{\mathrm{d}\Phi_d}{\mathrm{d}t} = 0 , \qquad (10)$$

where r_d , i_d , Φ_d are the resistance, the current and the magnetizing flux of the faulty phase.

We determine the short-circuit factor k_{cc} as:

$$k_{cc}[\%] = \frac{n_{cc}}{N_s} \cdot 100\%$$
, (11)

where N_s is the number of stator-turns; n_{cc} is the number of short-circuited turns.

The stator fluxes matrix is:

$$[\boldsymbol{\Phi}_{sc}] = [T_c] \cdot [\boldsymbol{\Phi}_s], \tag{12}$$

with

$$[T_c] = \begin{bmatrix} 1 & -1 & 0 & 0 \\ 0 & 1 & -1 & 0 \\ -1 & 0 & 1 & 0 \\ 0 & 0 & 0 & 1 \end{bmatrix};$$
 (13)

$$[\boldsymbol{\Phi}_{s}] = -[\boldsymbol{L}_{ss}] \cdot [\boldsymbol{i}_{sc}] - [\boldsymbol{L}_{sr}] \cdot [\boldsymbol{i}_{r}], \qquad (14)$$

where $[T_c]$ is the transformation matrix; $[L_{ss}]$ is the matrix of the stator inductances; $[L_{sr}]$ is the matrix of the stator and rotor mutual inductances; $[i_r]$ is the rotor currents vector.

In the case of an inter-turn fault in phase A, the stator and mutual inductances are given as:

$$[\mathbf{L}_{ss}] = \begin{bmatrix} b^{2} \cdot L_{s} & -b \cdot \frac{L_{ms}}{2} & -b \cdot \frac{L_{ms}}{2} & b \cdot f_{a} \cdot Lm_{s} \\ -b \cdot \frac{L_{ms}}{2} & L_{s} & -\frac{L_{ms}}{2} & -f_{a} \cdot \frac{L_{ms}}{2} \\ -b \cdot \frac{L_{ms}}{2} & -\frac{L_{ms}}{2} & L_{s} & -f_{a} \cdot \frac{L_{ms}}{2} \\ b \cdot f_{a} \cdot L_{ms} & -f_{a} \cdot \frac{L_{ms}}{2} & -f_{a} \cdot \frac{L_{ms}}{2} & f_{a}^{2} \cdot L_{s} \end{bmatrix}; (15)$$

$$[\mathbf{L}_{sr}] = L_{sr} \cdot \begin{bmatrix} M \\ f_{a} \end{bmatrix}, \qquad (16)$$

with

$$[\mathbf{M}] = \begin{bmatrix} b \cdot \cos(\theta) & b \cdot \cos\left(\theta + \frac{2 \cdot \pi}{3}\right) & b \cdot \cos\left(\theta - \frac{2 \cdot \pi}{3}\right) \\ \cos\left(\theta - \frac{2 \cdot \pi}{3}\right) & \cos(\theta) & \cos\left(\theta + \frac{2 \cdot \pi}{3}\right) \\ \cos\left(\theta + \frac{2 \cdot \pi}{3}\right) & \cos\left(\theta - \frac{2 \cdot \pi}{3}\right) & \cos(\theta) \end{bmatrix}; (17)$$

$$[f_{\theta}] = \left[f_a \cdot \cos(\theta) \quad f_a \cdot \cos\left(\theta + \frac{2 \cdot \pi}{3}\right) \quad f_a \cdot \cos\left(\theta - \frac{2 \cdot \pi}{3}\right) \right]; (18)$$

$$b = (1 - f_a); L_s = (L_{ms} + L_{ls}),$$
 (19)

where L_{ls} is the leakage inductance of the stator windings; L_{ms} is the stator magnetization inductance; L_{sr} is the maximum of the stator and rotor mutual inductances; f_a is the short-circuit factor.

The rotor voltages equation, based on equivalent rotor variables, is formulated as:

$$\frac{\mathrm{d}[\boldsymbol{\phi}_r]}{\mathrm{d}t} = [\boldsymbol{V}_r] + [\boldsymbol{R}_r] \cdot [\boldsymbol{i}_r], \qquad (20)$$

where $[V_r]$ is the rotor voltages vector; $[R_r]$ is the rotor winding resistances matrix; $[\boldsymbol{\Phi}_r]$ is the rotor fluxes vector:

$$[\boldsymbol{\Phi}_{r}] = -[\boldsymbol{L}_{rs}] \cdot [\boldsymbol{i}_{s}] - [\boldsymbol{L}_{rr}] \cdot [\boldsymbol{i}_{r}], \tag{21}$$

where $[L_{rs}] = [L_{sr}]^T$ is the rotor and stator mutual inductances matrix; $[L_{rr}]$ is the rotor inductances matrix.

The stator currents vector comprises 4 interdependent values, with only 3 independent components required for its calculation. The current vector is defined with 3 components: i_{as} , i_{bs} , and i_d yielding the following matrix representation:

$$[\mathbf{i}_{sc}] = [\mathbf{B}_{sc}] \cdot [\mathbf{i}_{abds}].$$
 (22)

The stator flux is represented by a vector consisting of 3 independent components, defined as follows:

$$[\boldsymbol{\Phi}_{abds}] = [A_{sc}] \cdot [\boldsymbol{\Phi}_{s}], \tag{23}$$

with

$$\begin{bmatrix} \boldsymbol{A_{sc}} \end{bmatrix} = \begin{bmatrix} 1 & -1 & 0 & 0 \\ 0 & 1 & -1 & 0 \\ 0 & 0 & 0 & 1 \end{bmatrix}; \ \begin{bmatrix} \boldsymbol{B_{sc}} \end{bmatrix} = \begin{bmatrix} 1 & 0 & 0 \\ 0 & 1 & 0 \\ -1 & -1 & 0 \\ 0 & 0 & 1 \end{bmatrix}.$$

Using (15), (22) and (23), we obtain:

$$\begin{cases}
[\boldsymbol{\Phi}_{abds}] = [\boldsymbol{M}_{sc}] \cdot [\boldsymbol{i}_{abds}] + [\boldsymbol{M}_{src}] \cdot [\boldsymbol{i}_{r}]; \\
[\boldsymbol{\Phi}_{r}] = [\boldsymbol{M}_{tsc}] \cdot [\boldsymbol{i}_{abds}] + [\boldsymbol{L}_{rr}] \cdot [\boldsymbol{i}_{r}];
\end{cases} (24)$$

with

$$\begin{cases}
[M_{sc}] = [A_{sc}] \cdot [L_{ss}] \cdot [B_{sc}]; \\
[M_{src}] = [A_{sc}] \cdot [L_{sr}]; \\
[M_{rsc}] = [L_{rs}] \cdot [B_{sc}],
\end{cases} (25)$$

Based on (24), we get:

$$\begin{cases} [i_{abds}] = [C_{sc}] \cdot [\boldsymbol{\Phi}_{sr}]; \\ [i_r] = [C_{rc}] \cdot [\boldsymbol{\Phi}_{rs}], \end{cases}$$
(26)

with

$$\begin{bmatrix}
[C_{sc}] = -([M_{sc}] - [M_{src}] \cdot [L_{rr}]^{-1} \cdot [M_{rsc}])^{-1}; \\
[C_{rc}] = -([L_{rr}] - [M_{rsc}] \cdot [M_{sc}]^{-1} \cdot [M_{src}])^{-1}; \\
[\boldsymbol{\Phi}_{sr}] = ([\boldsymbol{\Phi}_{abds}] - [M_{src}] \cdot [L_{rr}]^{-1} \cdot [\boldsymbol{\Phi}_{r}]) \\
[\boldsymbol{\Phi}_{rs}] = ([\boldsymbol{\Phi}_{r}] - [M_{rsc}] \cdot [M_{sc}]^{-1} \cdot [\boldsymbol{\Phi}_{abds}])
\end{bmatrix}$$

Finally, by using (7), (8), (20) and (26), we obtain the state model of DFIG:

$$\frac{d\left[\frac{\boldsymbol{\Phi}_{sc}}{dt}\right]}{dt} = \left[\boldsymbol{R}_{sc}\right] \cdot \left[\boldsymbol{B}_{sc}\right] \cdot \left[\boldsymbol{C}_{sc}\right] \cdot \left[\boldsymbol{\Phi}_{sr}\right] + \left[\boldsymbol{V}_{s}\right];$$

$$\frac{d\left[\boldsymbol{\Phi}_{r}\right]}{dt} = \left[\boldsymbol{R}_{r}\right] \cdot \left[\boldsymbol{C}_{rc}\right] \cdot \left[\boldsymbol{\Phi}_{rs}\right] + \left[\boldsymbol{V}_{r}\right];$$

$$\frac{d\Omega_{m}}{dt} = \frac{1}{J} \cdot \left(T_{em} - T_{m} - f_{v} \cdot \Omega_{m}\right).$$
(28)

The electromagnetic torque expression is:

$$T_{em} = p \cdot [\mathbf{i}_s]^t \cdot \frac{\partial [\mathbf{L}_{sr}]}{\partial \theta} \cdot [\mathbf{i}_r], \tag{29}$$

where p is the pole pairs number; θ is the mechanical angle (angle of the body rotation due to torque T_{em}).

Results. The simulations of the whole system were performed with MATLAB software. The wind turbine and DFIG parameters are given in Table 1, 2 with a short-circuit factor of 5 % on phase A. The wind speed and mechanical speed are shown in Fig. 1, 2. Figures 3–5 illustrate the stator currents, voltages and magnetic flux, while Fig. 6–8 show the spectrum analysis of the stator current I_{as} , voltage V_{as} and flux Φ_{as} .

Table 1
DFIG parameters

Di 10 parameters	
Rated power P_s , kW	4
Mutual inductance L_m , H	0.258
Stator inductance L_s , H	0.274
Rotor inductance L_r , H	0.303
Stator resistance R_s , Ω	4.85
Rotor resistance R_r , Ω	3.805
Number of pole pairs p	2
Moment of the inertia J , kg·m ²	0.045
Viscous friction f_v , kg·m ² ·s ⁻¹	0.0038

Table 2

Wind turbine parameters

will turblic parameters	
Radius R, m	3
Gear box ratio <i>G</i>	5.4
Number of blades n_p	3
Nominal wind speed v, m/s	12 m/s

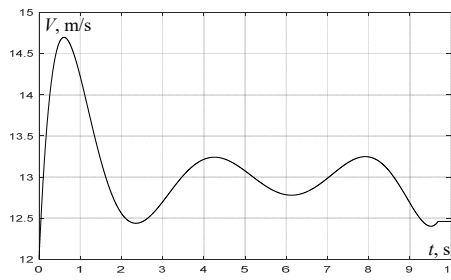
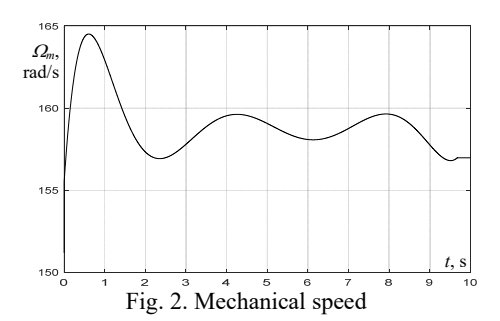


Fig. 1. Wind speed



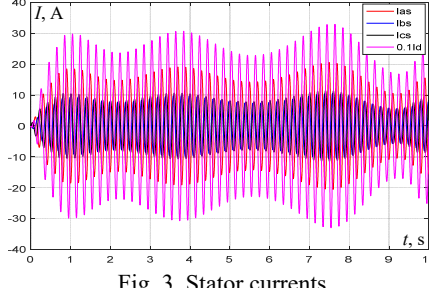


Fig. 3. Stator currents

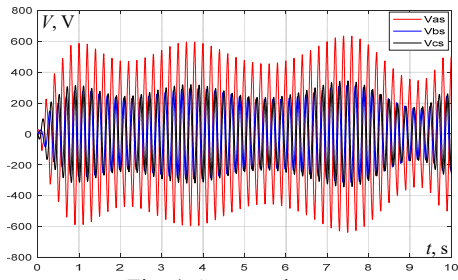


Fig. 4. Stator voltages

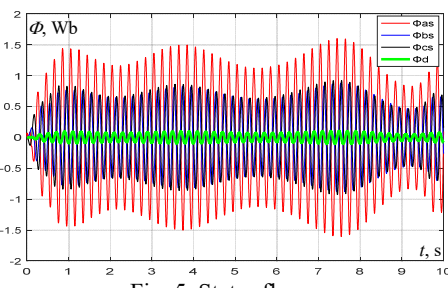


Fig. 5. Stator fluxes

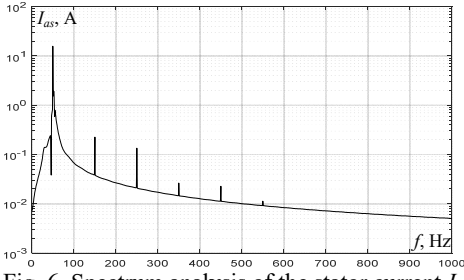


Fig. 6. Spectrum analysis of the stator current I_{as}

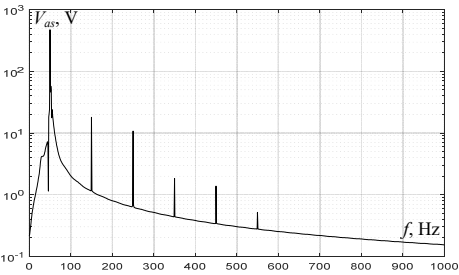


Fig. 7. Spectrum analysis of the stator voltage V_{as}

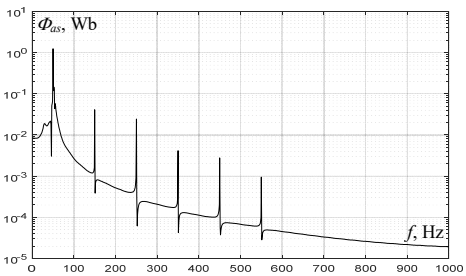


Fig. 8. Spectrum analysis of the stator flux Φ_{as}

Spectral analysis of these magnetic fluxes reveals significant variations when a 5 % inter-turn short-circuit occurs in phase A. At the same time, high-frequency components appear in the stator currents, producing acoustic noise and vibration. These phenomena induce additional stresses in the gearbox and turbine blades, reducing their service life. The stator current spectrum analysis reveals the emergence of distinct harmonics at frequencies of 150 Hz, 250 Hz and 350 Hz. These harmonics resemble those of stator flux and voltage. Harmonic components in the stator currents lead to the production of pulsating torques. As a result, significant consequences such as overheating occur, indicating that overcurrent is generated among the short-circuited turns and the stator windings, especially within the defective winding. Moreover, unbalanced voltages are generated in the stator windings as a result of the asymmetry of the stator fluxes. This asymmetry can adversely affect the control algorithms of the DFIG and disrupt the maximum power point tracking leading to a reduction in energy efficiency and stability.

Conclusions. This study analyzed the effect of stator inter-turn short-circuit faults on the operation of DFIGs in wind power systems, using a simplified electromagnetic model that includes the rise of neutral point voltage.

The model, based on line-to-line voltages, proved effective in identifying key fault-related harmonics through spectral analysis, confirming its diagnostic capability.

Simulation results showed that such faults lead to electromagnetic imbalances, which cause mechanical vibrations and control instability, ultimately reducing system reliability.

The proposed modeling approach offers a practical tool for condition monitoring and lays the groundwork for further studies on other fault types in DFIG-based wind turbines.

Conflict of interest. The authors declare that they have no conflicts of interest.

REFERENCES

- 1. Ma Y., Zhu D., Zou X., Kang Y., Guerrero J.M. Transient Characteristics and Quantitative Analysis of Electromotive Force for DFIG-based Wind Turbines during Grid Faults. Chinese Journal of Electrical Engineering, 2022, vol. 8, no. 2, pp. 3-12. doi: https://doi.org/10.23919/CJEE.2022.000010.
- 2. Rolan A., Bogarra S., Bakkar M. Integration of Distributed Energy Resources to Unbalanced Grids Under Voltage Sags With Grid Code Compliance. IEEE Transactions on Smart Grid, 13, 2022, vol. no. 1. pp. 355-366. https://doi.org/10.1109/TSG.2021.3107984.
- 3. Husari F., Seshadrinath J. Incipient Interturn Fault Detection and Severity Evaluation in Electric Drive System Using Hybrid HCNN-SVM Based Model. IEEE Transactions on Industrial Informatics, 2022, vol. 18, no. 3, pp. 1823-1832. doi: https://doi.org/10.1109/TII.2021.3067321.
- 4. Chen Y., Rehman A.U., Zhao Y., Wang L., Wang S., Zhang M., Zhao Y., Cheng Y., Tanaka T. Numerical Modeling, Electrical Characteristics Analysis and Experimental Validation of Severe Inter-Turn Short Circuit Fault Conditions on Stator Winding in DFIG of Wind Turbines. IEEE Access, 2021, vol. 9, pp. 13149-13158. doi: https://doi.org/10.1109/ACCESS.2021.3050876.
- 5. Sotoudeh A., Rezaei M.M. An adaptive control strategy for grid-forming of SCIG-based wind energy conversion systems. Energy Reports, 2023, vol. 10, pp. 114-122. https://doi.org/10.1016/j.egyr.2023.06.030

- 6. Huang S., Wang J., Huang C., Zhou L., Xiong L., Liu J., Li P. A fixed-time fractional-order sliding mode control strategy for power quality enhancement of PMSG wind turbine. *International Journal of Electrical Power & Energy Systems*, 2022, vol. 134, art. no. 107354. doi: https://doi.org/10.1016/j.ijepes.2021.107354.
- 7. Zhao S., Chen Y., Rehman A.U., Liang F., Wang S., Zhao Y., Deng W., Ma Y., Cheng Y. Detection of Interturn Short-Circuit Faults in DFIGs Based on External Leakage Flux Sensing and the VMD-RCMDE Analytical Method. *IEEE Transactions on Instrumentation and Measurement*, 2022, vol. 71, pp. 1-12. doi: https://doi.org/10.1109/TIM.2022.3186061.
- 8. Sarma N., Tuohy P.M., Djurovic S. Stator Electrical Fault Detection in DFIGs Using Wide-Band Analysis of the Embedded Signals From the Controllers. *IEEE Transactions on Energy Conversion*, 2021, vol. 36, no. 2, pp. 800-811. doi: https://doi.org/10.1109/TEC.2020.3017443.
- 9. Gurusamy V., Capolino G.-A., Akin B., Henao H., Romary R., Pusca R. Recent Trends in Magnetic Sensors and Flux-Based Condition Monitoring of Electromagnetic Devices. *IEEE Transactions on Industry Applications*, 2022, vol. 58, no. 4, pp. 4668-4684. doi: https://doi.org/10.1109/TIA.2022.3174804.
- 10. Botha S., Gule N. Vibrational Analysis of an Unbalanced Brushless Doubly Fed Induction Machine. 2023 IEEE International Electric Machines & Drives Conference (IEMDC), 2023, pp. 1-6. doi: https://doi.org/10.1109/IEMDC55163.2023.10239081.
- 11. Sahin I., Keysan O. Model Predictive Controller Utilized as an Observer for Inter-Turn Short Circuit Detection in Induction Motors. *IEEE Transactions on Energy Conversion*, 2021, vol. 36, no. 2, pp. 1449-1458. doi: https://doi.org/10.1109/TEC.2020.3048071.
- 12. Abid M., Laribi S., Larbi M., Allaoui T. Diagnosis and localization of fault for a neutral point clamped inverter in wind energy conversion system using artificial neural network technique. *Electrical Engineering & Electromechanics*, 2022, no. 5, pp. 55-59. doi: https://doi.org/10.20998/2074-272X.2022.5.09.
- 13. Alipoor G., Mirbagheri S.J., Moosavi S.M.M., Cruz S.M.A. Incipient detection of stator inter-turn short-circuit faults in a doubly-fed induction generator using deep learning. *IET Electric Power Applications*, 2023, vol. 17, no. 2, pp. 256-267. doi: https://doi.org/10.1049/elp2.12262.
- 14. Toshani H., Abdi S., Hosseini N.K., Abdi E. Fault Diagnosis of Squirrel Cage Induction Generator for Wind Turbine Applications Using a Hybrid Deep Neural Network and Decision Tree Approach. 2021 International Conference on Electrical, Computer and Energy Technologies (ICECET), 2021, pp. 1-6. doi: https://doi.org/10.1109/ICECET52533.2021.9698556.
- 15. St-Onge X.F., Cameron J., Saleh S., Scheme E.J. A Symmetrical Component Feature Extraction Method for Fault Detection in Induction Machines. *IEEE Transactions on Industrial Electronics*, 2019, vol. 66, no. 9, pp. 7281-7289. doi: https://doi.org/10.1109/TIE.2018.2875644.
- 16. Mellah H., Arslan S., Sahraoui H., Hemsas K.E., Kamel S. The Effect of Stator Inter-Turn Short-Circuit Fault on DFIG Performance Using FEM. Engineering, Technology & Applied Science Research, 2022, vol. 12, no. 3, pp. 8688-8693. doi: https://doi.org/10.48084/etasr.4923.
- 17. Ahmadpour A., Dejamkhooy A., Shayeghi H. Fault Diagnosis of HTS–SLIM Based on 3D Finite Element Method and Hilbert–Huang Transform. *IEEE Access*, 2022, vol. 10, pp. 35736-35749. doi: https://doi.org/10.1109/ACCESS.2022.3159693.

- 18. Grechko O.M. Influence of the poles shape of DC electromagnetic actuator on its thrust characteristic. *Technical Electrodynamics*, 2024, no. 1, pp. 38-45. doi: https://doi.org/10.15407/techned2024.01.038.
- 19. Diboune Y., Hachelaf R., Kouchih D. Theoretical and experimental analysis of unbalanced doubly fed induction generators. *IAES International Journal of Robotics and Automation (IJRA)*, 2024, vol. 13, no. 4, pp. 476-484. doi: https://doi.org/10.11591/ijra.v13i4.pp476-484.
- 20. Alphan H. Modelling potential visibility of wind turbines: A geospatial approach for planning and impact mitigation. Renewable and Sustainable Energy Reviews, 2021, vol. 152, art. no. 111675. doi: https://doi.org/10.1016/j.rser.2021.111675.
- 21. Sajan C., Satish Kumar P., Virtic P. Enhancing grid stability and low voltage ride through capability using type 2 fuzzy controlled dynamic voltage restorer. *Electrical Engineering & Electromechanics*, 2024, no. 4, pp. 31-41. doi: https://doi.org/10.20998/2074-272X.2024.4.04.
- **22.** Nid A., Sayah S., Zebar A. Power fluctuation suppression for grid connected permanent magnet synchronous generator type wind power generation system. *Electrical Engineering & Electromechanics*, 2024, no. 5, pp. 70-76. doi: https://doi.org/10.20998/2074-272X.2024.5.10.
- 23. Muthukaruppasamy S., Dharmaprakash R., Sendilkumar S., Parimalasundar E. Enhancing off-grid wind energy systems with controlled inverter integration for improved power quality. *Electrical Engineering & Electromechanics*, 2024, no. 5, pp. 41-47. doi: https://doi.org/10.20998/2074-272X.2024.5.06.
- 24. Kaddache M., Drid S., Khemis A., Rahem D., Chrifi-Alaoui L. Maximum power point tracking improvement using type-2 fuzzy controller for wind system based on the double fed induction generator. *Electrical Engineering & Electromechanics*, 2024, no. 2, pp. 61-66. doi: https://doi.org/10.20998/2074-272X.2024.2.09.
- 25. Mousavi Y., Bevan G., Kucukdemiral I.B., Fekih A. Sliding mode control of wind energy conversion systems: Trends and applications. *Renewable and Sustainable Energy Reviews*, 2022, vol. 167, art. no. 112734. doi: https://doi.org/10.1016/j.rser.2022.112734.
- **26.** Kong X., Ma L., Liu X., Abdelbaky M.A., Wu Q. Wind Turbine Control Using Nonlinear Economic Model Predictive Control over All Operating Regions. *Energies*, 2020, vol. 13, no. 1, art. no. 184. doi: https://doi.org/10.3390/en13010184.
- 27. L'Hadj Said M., Ali Moussa M., Bessaad T. Control of an autonomous wind energy conversion system based on doubly fed induction generator supplying a non-linear load. *Electrical Engineering & Electromechanics*, 2025, no. 4, pp. 3-10. doi: https://doi.org/10.20998/2074-272X.2025.4.01.

Received 09.02.2025 Accepted 26.05.2025 Published 02.11.2025

Y. Diboune¹, PhD Student,

R. Hachelaf¹, Assistant Professor,

D. Kouchih¹. PhD. Associate Professor.

Automatic and Electrotechnics Department,

Electrical Systems and Remote-Control Laboratory (LabSET), Faculty of Technology, University of Blida 1, Algeria, e-mail: yaakoubd479@gmail.com (Corresponding Author);

haclefr@yahoo.fr; djkouchih@yahoo.fr

How to cite this article:

Diboune Y., Hachelaf R., Kouchih D. Effect of short-circuit in stator windings on the operation of doubly-fed induction generators operating in a wind power system. *Electrical Engineering & Electromechanics*, 2025, no. 6, pp. 3-7. doi: https://doi.org/10.20998/2074-272X.2025.6.01